Crystal scintillators for high precision beta spectroscopy: the GAIAS experiment

Dr. Alice Leoncini, PhD in Physics
Department of Physics, University of Rome "Tor Vergata",
INFN – Rome Tor Vergata

GAIAS
GAxIal Analysis with Scintillators

LNGS, July 09th 2026

Why constrain the nuclear axial response?

Effective value of the weak coupling g_A is involved in all weak processes. and depends on the transferred momentum $\boldsymbol{q}$. It has impact on:

- studies of rare β decays ($g_A^{eff}(q \to 0)$)
- processes in neutrino physics (**$0\nu\beta\beta$ decay**, medium-energy (anti)neutrino-nucleus scattering, nuclear muon capture, ...) ($g_A^{eff}(q\sim 100 \text{ MeV})$)
- processes in astrophysics (allowed and forbidden β decays, low-energy (anti)neutrino-nucleus scattering cross sections, ...) ($g_A^{eff}(q\sim 0)$)

g_A^{eff} is not a universal constant, but a model-dependent way to encode possible missing correlations, restricted model spaces, two-body currents and medium effects.

Affects strongly the determination of neutrino properties!

Why constrain the nuclear axial response?

- The observation of $\mathbf{0\nu\beta\beta}$ decay would prove lepton number violation and establish the Majorana nature of neutrinos.

- However, translating a measured half-life (limit) into information on the $m_{\beta\beta}$ requires reliable calculations of nuclear matrix elements and a consistent treament of the axial current.

$$\left[T_{1/2}^{0\nu}\right]^{-1} = \left(g_A^{eff}\right)^4 G^{0\nu}\left|M^{0\nu}\right|^2 \left|\frac{\langle m_{\beta\beta}\rangle}{m_e}\right|^2$$

$M^{0\nu}$ nuclear matrix element (NME)
g_A^{eff} eff. axial-vector coup. const.
$G^{0\nu}$ phase-space factor
m_e electron mass
$\langle m_{\beta\beta}\rangle$ effective Majorana mass of the ν

- The experimentally measured quantity is $T_{1/2}^{0\nu}$. The uncertainty in g_A^{eff} and $M^{0\nu}$ affects the interpretation of $T_{1/2}^{0\nu}$ in terms of $m_{\beta\beta}$.

Why constrain the nuclear axial response?

Experimental input:
$T_{1/2}^{0\nu}$ limit/sensitivity
determined by isotope mass, exposure, efficiency, energy resolution, long-term stability, background.

→

Nuclear-theory input:
$M^{0\nu}$, axial current, g_A^{eff}
affected by nuclear correlations, model-space truncation, two-body currents and medium effects.

→

Physics output:
$\langle m_{\beta\beta} \rangle$ constraint
limited by nuclear-model uncertainties, which increases further due to the uncertainty of the g_A quenching.

A dedicated experimental effort is needed to constrain g_A^{eff}, since no clear consensus has been reached.

Theoretical background

Weak Hamiltonian (leptonic-hadronic): $\boldsymbol{H_W = \frac{G_F}{\sqrt{2}}\left(j_{L\mu} J_L^{\mu+}\right) + \mathrm{h.c.}}$

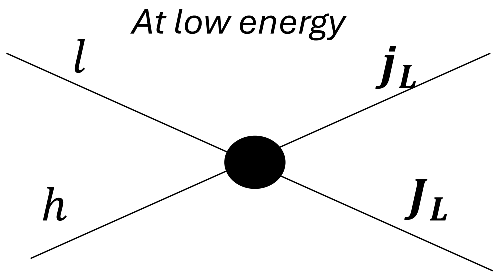

- $G_F = 1.16637 \times 10^{-5}$ GeV^{-2} is the Fermi coupling constant;
- $j_{L\mu} = \bar{e}\gamma_\mu(1-\gamma_5)\nu_{e,L}$, where $\nu_{e,L} = \sum_{i=1}^{3} U_{ei} N_{iL}$.
- At the quark level: $J_L^{\mu+} = \bar{u}\gamma^\mu(1-\gamma_5)d$ → at the hadronic level: $\boldsymbol{J_L^{\mu+} = \bar{p}\,[V^\mu - A^\mu]n}$

Vector current:

$$V^\mu = g_V(q^2)\gamma^\mu + i g_M(q^2)\frac{\sigma^{\mu\nu}}{2m_N} q_\nu,$$

Axial-vector current:

$$A^\mu = g_A(q^2)\gamma^\mu\gamma_5 + g_P(q^2) q^\mu \gamma_5$$

Where m_N is the nucleon mass (roughly 1 GeV), $g_M(q^2)$ is the weak—magnetism form factor and $g_P(q^2)$ is the induced pseudoscalar form factor.

Vector and axial-vector coupling constants

In the hypothesis of conserved vector-current (CVC) and partially conserved axial-vector-current (PCAC), the free-nucleon values are:

$$g_V = 1.00 \qquad g_A^{free} = 1.2723(23) \text{ [1]}$$

Inside nuclear matter, g_V remains equal to 1, while the value of g_A is affected by many-nucleon correlations $\Rightarrow$ its value might be quenched or enhanced:

$$g_A^{eff} = \mathrm{q}_A \cdot g_A^{free}$$

where $\mathbf{q}_A$ is a quenching parameter.

[1] Suhonen JT (2017), Front. Phys. 5:55.

The weak axial coupling constant g_A

g_A^{eff} can be affected by:

- meson-exchange currents
- nuclear medium effects (interference of non-nucleonic degrees of freedom)
- nuclear model effects (many-body approaches: ISM, IBM-2, QRPA)

$\Rightarrow$ In the interpretation of the experimental data, these effects are difficult to disentangle without model-dependent assumptions.

Dependence of g_A^{eff} on the mass number for different nuclear models

Results for $g_A^{eff}(q \to 0)$ from the GT $\beta^{\pm}$/EC and $2\nu\beta\beta$ calculations

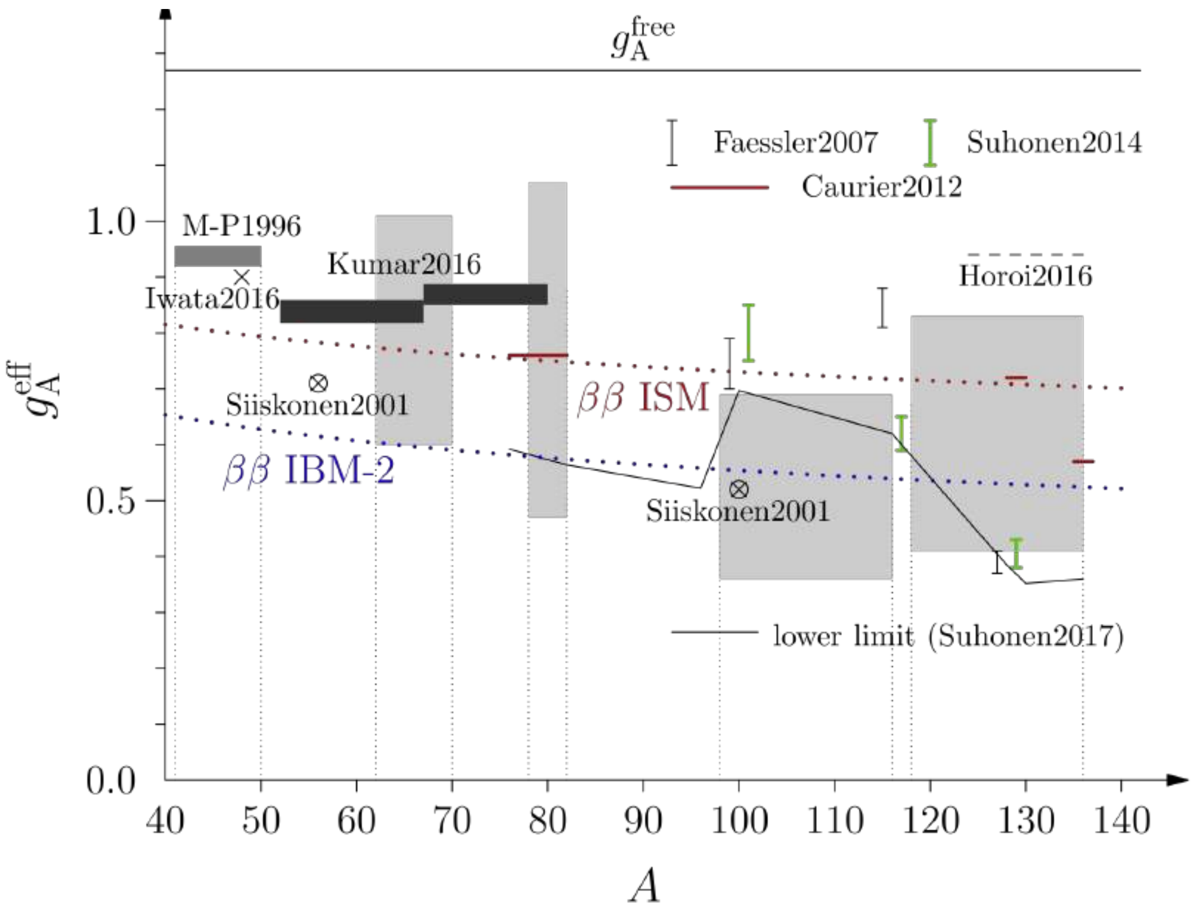

[2] H. Ejiri, J. Suhonen and K. Zuber, Physics Reports 797 (2019) 1

- **Faessler2007**: pnQRPA A. Faessler et al., arXiv 0711.3996v1 [Nucl-th]
- **Suhonen2014**: pnQRPA J. Suhonen et al., Nucl. Phys. A 924 (2014) 1
- **Suhonen2017**: pnQRPA J. Suhonen, Phys. Rev. C 96 (2017) 055501
- **Caurier2012**: ISM E. Caurier et al., Phys. Lett. B 711 (2012) 62
- **Horoi2016**: ISM M. Horoi et al., Phys.
- Rev. C 93 (2016) 024308
- **M-P1996**: ISM G. Martínez-Pinedo et al., Phys. Rev. C 53 (1996) R2602
- **Iwata2016**: ISM Y. Iwata et al., Phys. Rev. Lett. 116 (2016) 112502
- **Kumar2016**: ISM V. Kumar et al., J. Phys. G 43 (2016) 105104
- **Siiskonen2001**: ISM T. Siiskonen et al., Phys. Rev. C 63 (2001) 055501
- **ββISM and IBM-2**: J. Barea et al., Phys. Rev. C 87 (2013) 014315
- **Light hatched regions**: pnQRPA H. Ejiri et al., J. Phys. G 42 (2015) 055201 ; P. Pirinen et al., Phys. Rev. C 91 (2015) 054309 ; F. Deppisch et al., Phys. Rev. C 94 (2016) 055501.

Probing g_A^{eff} through nuclear observables

Nuclear Process	Momentum transfer	Main g_A dependence	Experimental observable
β decay transition (allowed GT)	few MeV	$(g_A^{eff})^2$	$T_{1/2}^{\beta}$, branching ratios but constrained by NMEs calculations
Forbidden non-unique β decay	few MeV	g_A^{eff} and $(g_A^{eff})^2$	β spectral shape using **Spectrum-Shape Method (SSM)** [3]
$2\nu\beta\beta$ decay	few MeV	$(g_A^{eff})^4$	$T_{1/2}^{2\nu}$ but constrained by NMEs calculations
Double charge-exchange reactions	~10 - 100 MeV	No direct g_A^{eff} scaling; indirect constraint on spin–isospin NMEs relevant to $0\nu\beta\beta$	DCE differential cross sections and angular distributions
Neutrino interaction with matter (low-energy (anti)neutrino-nucleus scattering, nuclear muon capture, ...)	~10 - 100 MeV	g_A^{eff} or $(g_A^{eff})^2$	Cross sections, capture rates but constrained by the NMEs calculations

[3] M. Haaranen, P. C. Srivastava and J. Suhonen, Phys. Rev. C 93 (2016) 034308

Probing g_A^{eff} in nuclear weak processes

Nuclear Process	Momentum transfer	Main g_A dependence	Experimental observable
β decay transition (allo			nching ratios but ed by NMEs ons
Forbidden non-uniqu			shape using **n-Shape Method**
2n2b decay			onstrained by NMEs ons
0n2b decay			onstrained by NMEs ons and $\langle m_\nu \rangle$
Neutrino interaction (low-energy (anti)neut nucleus scattering, nuc capture, ...)			ctions, capture rates trained by the NMEs ations

Forbidden β decays probe the low-momentum axial response of nuclei. They do not directly determine the $0\nu\beta\beta$ NME, but provide key experimental constraints for nuclear models and for the treatment of g_A^{eff}.

[2] M. Haaranen, P. C. Srivastava and J. Suhonen, Phys. Rev. C 93 (2016) 034308

Classification of β decays

They are classified as ***allowed*** or ***forbidden*** with some level of forbiddenness depending on the change of spin J and parity π between parent and daughter nuclei.

Transition type	$\Delta J^{\Delta\pi}$	$\Delta\pi$	Forbiddeness
Allowed	$0^+, 1^+$		
Forbidden unique	$2^-, 3^+, 4^-, \ldots$	$(-1)^{\Delta J - 1}$	$\Delta J - 1$
Forbidden non-unique	$1^-, 2^+, 3^-, 4^+, \ldots$	$(-1)^{\Delta J}$	ΔJ

Angular momentum in the β decay:

$\vec{J}_i = \vec{J}_f + \vec{L} + \vec{S}$; with $\vec{L} = \vec{l}_e + \vec{l}_\nu$ and $\vec{S} = \vec{s}_e + \vec{s}_\nu$

Parity change: $\Delta\pi = (-1)^L$

- **Allowed** decays if $|\vec{L}| = 0$
- **Forbidden** decays if $|\vec{L}| > 0$
- **Fermi** decays (F) if $|\vec{S}| = 0$
- **Gamow-Teller** decays (GT) if $|\vec{S}| = 1$

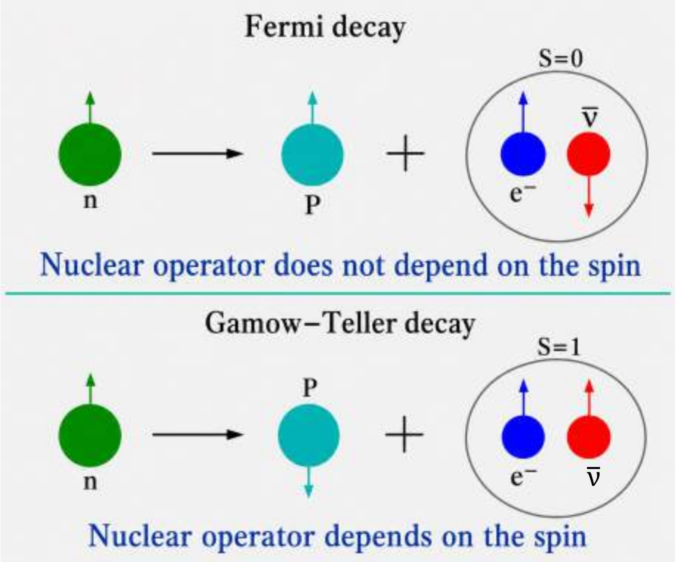

In forbidden decays, the total change in angular momentum is:

- In forbidden unique (FU) beta decay $\Rightarrow$ $\Delta J = L + 1$
- In forbidden non-unique (FNU) beta decay $\Rightarrow$ $\Delta J = L - 1$ or $\Delta J = L$

Beta-spectrum shapes in forbidden β decays

The expected energy spectrum of the electrons has different dependence on the value of g_A:

- FU transitions, at leading order the spectrum is proportional to g_A^2:

$$\frac{dR}{dE_e} \sim g_A^2 \; f(E_e) \quad \Longrightarrow \quad T_{1/2} \sim g_A^{-2}$$

- FNU transitions, at leading order the spectrum has a complicated dependence on g_A:

$$\frac{dR}{dE_e} \sim g_V^2 \; f_V(E_e) + 2 g_V g_A f_{VA}(E_e) + g_A^2 \, f_A(E_e)$$

- The unique decays (**FU**) have (essentially) **universal** β spectrum shapes with a **weak** nuclear-structure dependence.
- The non-unique decays (**FNU**) can show **strong** dependence on the details of nuclear structure and hence the associated β spectra are not universal.

FNU β decays as a probe for g_A^{eff}:

Spectrum-Shape Method (SSM)

$$\frac{dR}{dE_e} \sim g_V^2\ f_V(E_e) + 2 g_V g_A f_{VA}(E_e) + g_A^2\ f_A(E_e)$$

1. Measure high-statistics β spectrum with low background.

2. Compute theoretical spectra for different g_A^{eff} values.

3. Compare experimental β spectrum with the theoretical one.

4. Extract g_A^{eff}, best-fit comparison with data + cross-check among different nuclear models

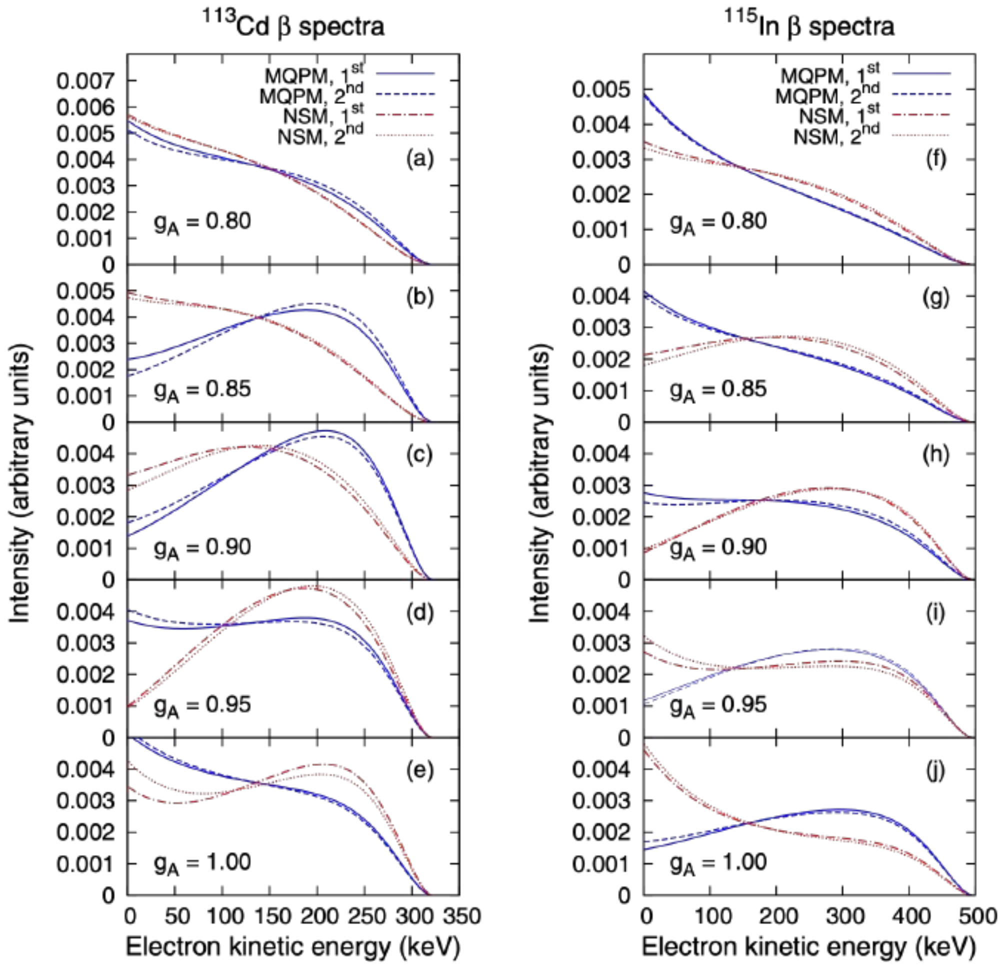

[3] M. Haaranen, P. C. Srivastava and J. Suhonen, Phys. Rev. C 93 (2016) 034308

List of some non-unique β decay transitions and their sensitivity to the value of g_A - part I

Transition	$J_i^{\pi_i}$ (gs)	$J_f^{\pi_f}(n_f)$	Branching	K	Sensitivity	Nuclear model
$^{50}V \rightarrow {}^{50}Cr$	6^+	2^+ (1)	~0	4	Weak	ISM
$^{59}Fe \rightarrow {}^{59}Co$	$3/2^-$	$7/2^-$ (gs)	0.18%	2	Moderate	ISM
$^{60}Fe \rightarrow {}^{60}Co$	0^+	2^+ (1)	**100%**	2	Moderate	ISM
$^{85}Br \rightarrow {}^{85}Kr$	$3/2^-$	$9/2^+$ (gs)	~0	3	Moderate	MQPM
$^{87}Rb \rightarrow {}^{87}Sr$	$3/2^-$	$9/2^+$ (gs)	**100%**	3	Moderate	MQPM, ISM
$^{94}Nb \rightarrow {}^{94}Mo$	6^+	4^+ (2)	**100%**	2	Strong	NSM
$^{96}Zr \rightarrow {}^{96}Nb$	0^+	6^+ (gs)	~0	6	Strong	ISM
$^{97}Zr \rightarrow {}^{97}Nb$	$1/2^+$	$9/2^+$ (gs)	~0	4	Strong	MQPM
$^{98}Tc \rightarrow {}^{98}Ru$	6^+	4^+ (3)	**100%**	2	Strong	ISM
$^{99}Tc \rightarrow {}^{99}Ru$	$9/2^+$	$5/2^+$ (gs)	**100%**	2	Strong	MQPM, ISM
$^{101}Mo \rightarrow {}^{101}Tc$	$1/2^+$	$9/2^+$ (gs)	~0	4	Strong	MQPM
$^{113}Cd \rightarrow {}^{113}In$	$1/2^+$	$9/2^+$ (gs)	**100%**	4	Strong	MQPM, ISM, IBFM-2
$^{113m}Cd \rightarrow {}^{113}In$	$11/2^-$	$9/2^+$ (gs)	**100%**	1	Strong	ISM, NSM

List of some non-unique β decay transitions and their sensitivity to the value of g_A - part II

Transition	$J_i^{\pi_i}$ (gs)	$J_f^{\pi_f}(n_f)$	Branching	K	Sensitivity	Nuclear model
$^{115}Cd \rightarrow {}^{115}In$	$1/2^+$	$9/2^+\ (gs)$	~ 0	4	**Strong**	MQPM
$^{115}In \rightarrow {}^{115}Sn$	$9/2^+$	$1/2^+\ (gs)$	**100%**	4	**Strong**	MQPM, ISM, IBFM-2
$^{117}Cd \rightarrow {}^{117}In$	$1/2^+$	$9/2^+\ (gs)$	~ 0	4	**Strong**	MQPM
$^{119}In \rightarrow {}^{119}Sn$	$9/2^+$	$1/2^+\ (gs)$	~ 0	4	**Strong**	MQPM
$^{123}Sn \rightarrow {}^{123}Sb$	$11/2^-$	$1/2^+\ (4)$	~ 0	5	**Weak**	MQPM
$^{136}Te \rightarrow {}^{136}I$	0^+	$(1^-)\ (\mathrm{gs})$	8.7%	1	**Strong**	ISM
$^{137}Xe \rightarrow {}^{137}Cs$	$7/2^-$	$5/2^+\ (1)$	30%	1	**Strong**	ISM
$^{138}Cs \rightarrow {}^{138}Ba$	3^-	$3^+\ (1)$	44%	1	**Strong**	ISM
$^{141}Ce \rightarrow {}^{141}Pr$	$7/2^-$	$5/2^+\ (\mathrm{gs})$	31%	1	**Weak**	MQPM
$^{210}Bi \rightarrow {}^{210}Po$	1^-	$0^+\ (\mathrm{gs})$	**100%**	1	**Strong**	ISM

Recent experimental studies on g_A^{eff}

Nuclear transition	Experimental approach	Nuclear model adopted	g_A^{eff}	Reference
$^{115}\mathrm{In}(9/2^+) \to {}^{115}\mathrm{Sn}(1/2^+)$ 4th FNU	ACCESS: InI cryogenic calorimeter	ISM best fit; MQPM, IBFM-2 cross-check	$0.964^{+0.010}_{-0.006}$	Pagnanini et al. PRL 133 (2024) 122501
$^{115}\mathrm{In}(9/2^+) \to {}^{115}\mathrm{Sn}(1/2^+)$ 4th FNU	High-resolution $LiInSe_2$ bolometer	ISM, IBM, MQPM	$0.830(2)–0.936(3)$	Leder et al. PRL 129 (2022) 232502
$^{113}\mathrm{Cd}(1/2^+) \to {}^{113}\mathrm{In}(9/2^+)$ 4th FNU	COBRA: CdZnTe semiconductor detectors at LNGS	ISM, MQPM, IBFM-2	$0.828(140)–0.993(63)$	Kostensalo et al. Phys. Lett. B 822 (2021) 136652
$^{113}\mathrm{Cd}(1/2^+) \to {}^{113}\mathrm{In}(9/2^+)$ 4th FNU	$CdWO_4$ bolometer at Canfranc (Spain)	NSM, MQPM, IBFM-2	$0.998(6)–1.160(19)$	Bandac et al. Eur. Phys. J. C (2024) 84:1158
$^{99}\mathrm{Tc}(9/2^+) \to {}^{99}\mathrm{Ru}(5/2^+)$ 2nd FNU	Artificial ^{99}Tc source embedded in a 4π Au absorber and measured with a Metallic Magnetic Calorimeter (MMC)	NSM, ISM, MQPM	1.0 – 1.2	Song et al, arXiv:2506.17544v1 [nucl-ex]
$^{99}\mathrm{Tc}(9/2^+) \to {}^{99}\mathrm{Ru}(5/2^+)$ 2nd FNU	ASPECT-BET: ^{99}Tc source deposited on Si substrate and measured with Silicon Drift Detector (SDD)	RSM	Not value quoted yet	Nava et al., Sensors 24 (2024) 8202
$^{113m}\mathrm{Cd}(11/2^-) \to {}^{113}\mathrm{In}(9/2^+)$ 1st FNU	**$^{106}CdWO_4$ crystal scintillator enriched in ^{106}Cd at 66% at LNGS**	**NSM/KSHELL**	≈ 0.80	**Belli et al. Phys. Rev. C 112 (2025) 045503**
$^{113}\mathrm{Cd}(1/2^+) \to {}^{113}\mathrm{In}(9/2^+)$ 4th FNU	**$^{106}CdWO_4$ crystal scintillator enriched in ^{106}Cd at 66% at LNGS**	**MQPM, ISM, IBFM-2**	≈ 0.90	**Belli et. al., Phys. Rev. C 76, (2007) 064603**
$^{87}\mathrm{Rb}(3/2^-) \to {}^{87}\mathrm{Sr}(9/2^+)$ 3rd FNU	**Rb_2ZrCl_6 crystal scintillator at LNGS**	**NSM + MQPM**	$\approx 0.40 - 0.60$	**Belli et al. EPJA 62 (2026) 16**

GAIAS

GAxIal Analysis with Scintillators

GAIAS studies g_A^{eff} through precision measurements of forbidden non-unique β decays using inorganic crystal scintillators as source-in-detector media.

1. Select isotope

high β branch, suitable Q_β, predicted sensitivity

2. Engineer crystal

natural content or controlled isotope incorporation

3. Measure spectrum

low-background setup and stable long-term operation

4. Extract g_A^{eff}

shape comparison with nuclear-model calculations

Crystal scintillators as source-in-detector materials for precision β spectroscopy

Crystal scintillators features	Impact on β-spectroscopy
«Source=detector» approach	allows β-emitting isotopes to be incorporated directly into the crystal bulk, providing high detection efficiency ($\varepsilon \approx 100\%$)
High light yield and good energy resolution	improve β spectral-shape reconstruction and help control detector-response distortions
Low energy threshold	enhances sensitivity to g_A^{eff}-dependent spectral-shape variations, especially in the low-energy ranges
Radiopurity	reduces background and simplifies full-spectrum modelling
Optical and mechanical stability	keeps gain, response and calibration under control
Chemical compatibility with β isotope	enables natural or controlled source incorporation

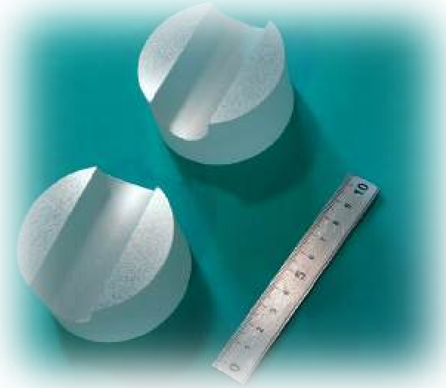

Experimental proof of concept: β decay of ^{113}Cd

Aim: To measure the β spectrum shape and $T_{1/2}$ of ^{113}Cd → ^{113}In **4th FNU decay** with accuracy better than those in previous experiments (4-12%)

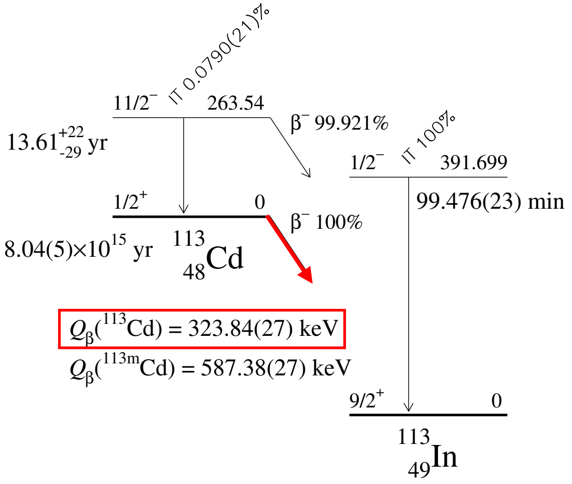

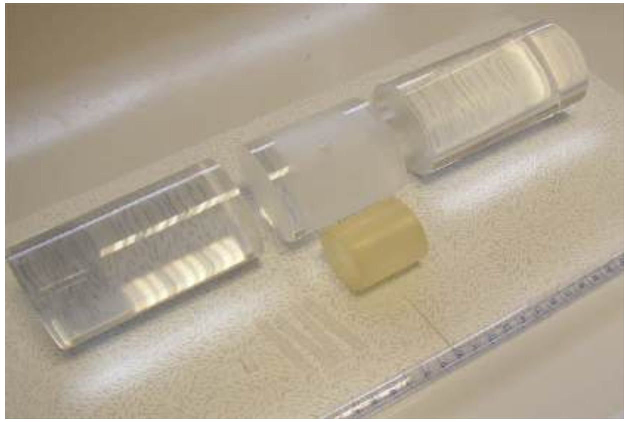

- Low-background crystal scintillator **$CdWO_4$** (⌀ 40 mm x 43 mm, mass of 434 g) → ^{113}Cd naturally present with $\delta \approx 12.2\%$.
- 10 years stored in the Solotvina underground Laboratory (Ukraine) on a depth of 1000 m w.e.
- The detector was measured in the low-background DAMA/R&D set-up at LNGS over 2758 h.
- Activity of ^{113}Cd: 558(4) mBq/kg.

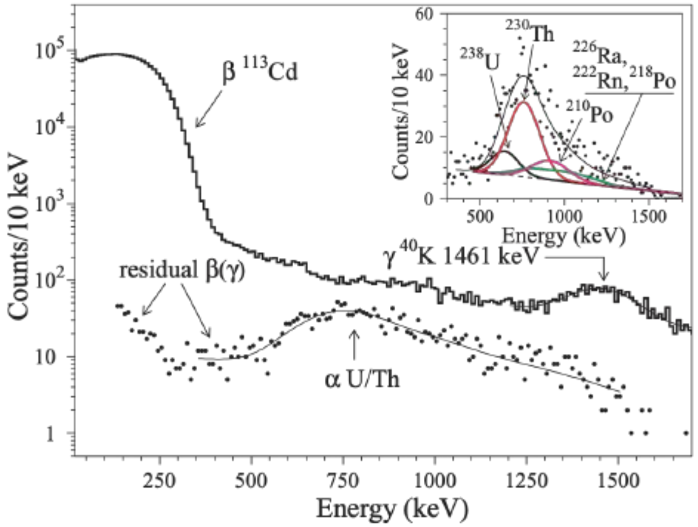

P. Belli et. al., Phys. Rev. C **76**, 064603 (2007)

β decay of ^{113}Cd : Results

1. $T_{1/2} = (8.04 \pm 0.05) \times 10^{15}$ yr (precision 0.6%)

2. Shape of spectrum: with the highest accuracy above the **energy threshold** $\approx$ **28 keV**.

The analytical β spectrum of ^{113}Cd obtained after deconvolution of the experimental β spectrum, with the uncertainties

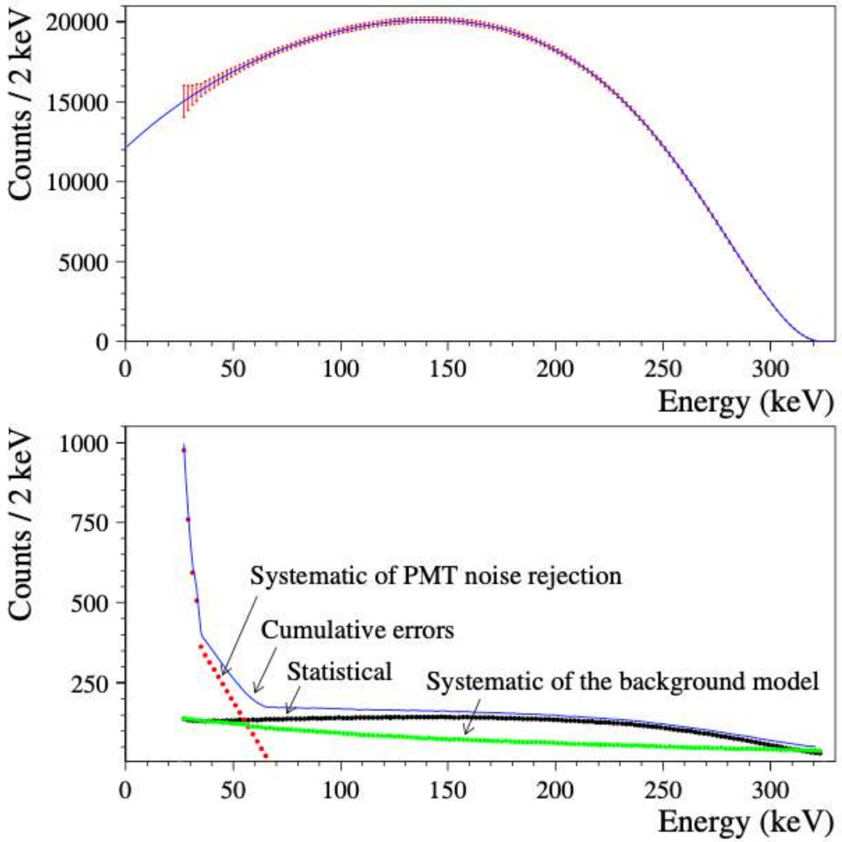

$g_A^{eff} \approx 0.90$

P. Belli et. al., Phys. Rev. C **76**, 064603 (2007)

P. Belli et al., Eur. Phys. J. A 55, 140 (2019).

Experimental proof of concept: β decay of ^{113m}Cd

Aim: to evaluate the $T_{1/2}$ of $^{113m}\mathbf{Cd}(11/2^-) \rightarrow {}^{113}\mathbf{In}(9/2^+)$ **1st FNU decay** by comparing counting rates from spectra measured several years apart.

- Low-background crystal scintillator ^{106}**CdWO$_4$** enriched in ^{106}Cd at 66%, mass of 215.5 g.

- ^{113m}**Cd origin (?):** maybe produced by neutron activation of the Cd material before the isotope enrichment. The residual ^{113}Cd isotopic fraction in the enriched crystal is $\delta(^{113}\mathrm{Cd}) = 3.935(3)\%$.

- Three different experimental campaigns: 2009, 2015 and 2023 in the DAMA/R&D and DAMA/CRYS setups at LNGS.

- **2023 upgrade**: removal of quartz light guides; new low-background PMTs; improved light collection efficiency; lowered **energy threshold down to 26 keV**; energy resolution $\sigma = 23.2(3)$ keV @587 keV.

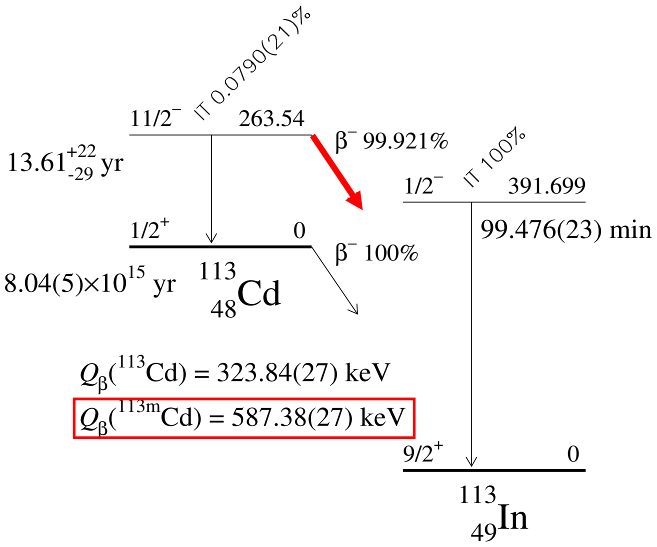

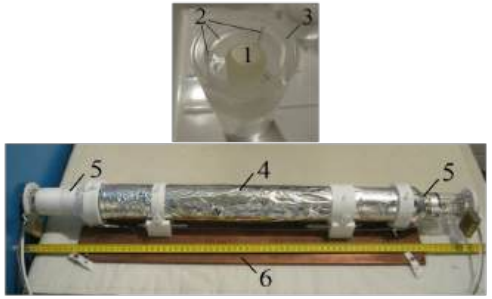

- Activity of ^{113m}Cd:
  - 131.91(16) Bq/kg in 2009;
  - 99.65(12) Bq/kg in 2015;
  - 64.72(8) Bq/kg in 2023.

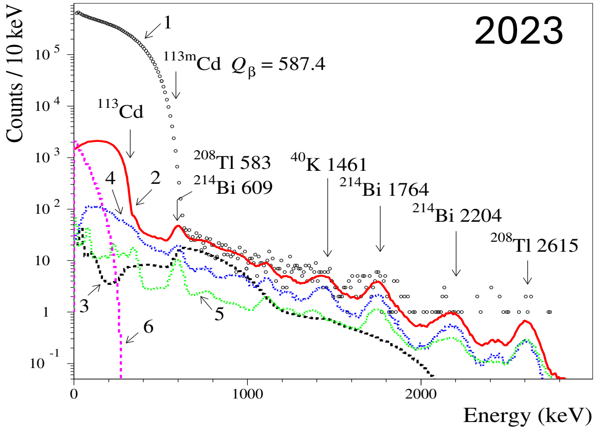

P. Belli et al. Phys. Rev. C 112 (2025) 045503

β decay of ^{113m}Cd: Results

Fit of the energy spectrum of β/γ events measured by the low-background $^{106}CdWO_4$ scintillation detector in 2023 (1) for 340.9 h in the energy interval E^{fit}_1 –E^{fit}_2 (26 – 600 keV).

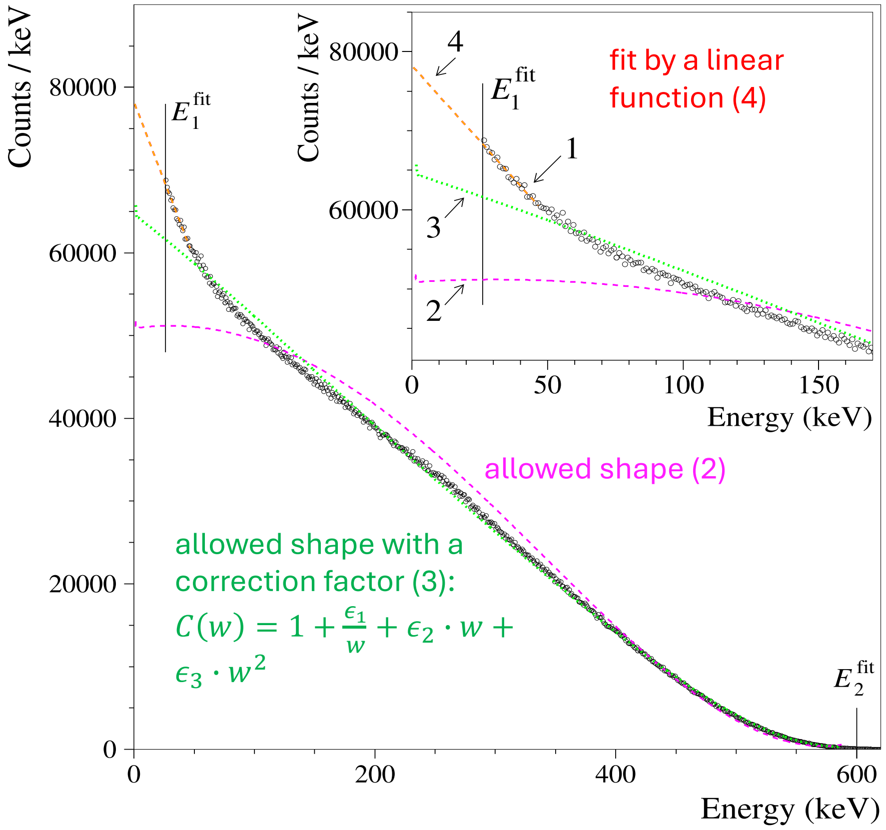

P. Belli et al. Phys. Rev. C 112 (2025) 045503

- Shell-model treatment shows that the spectral shape is sensitive to g_A ; low-energy atomic shell effects matter.
- Comparison with the considered models indicates that the data are best described assuming a quenched axial-vector coupling constant of $g_A \approx 0.8$.
- <u>A strong proof-of-principle, but not yet the final dedicated g_A determination.</u>

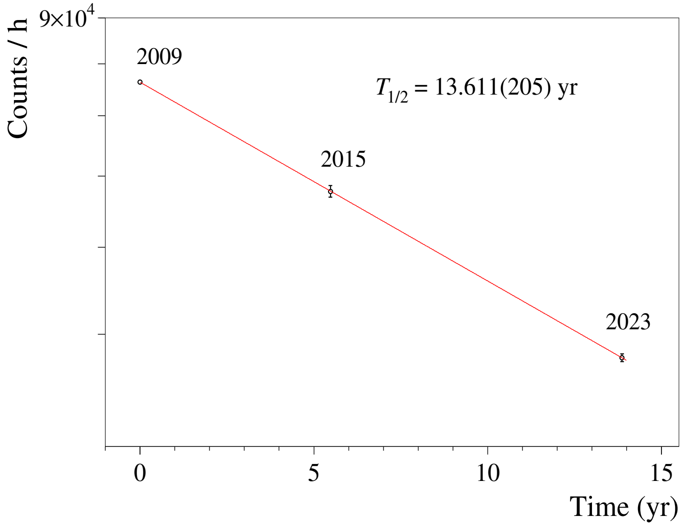

$T_{1/2} = 13.61^{+0.22}_{-0.29}$ yr

Experimental proof of concept: β decay of ^{87}Rb

Aim: to measure the spectral shape of $^{87}\mathbf{Rb}(3/2^-) \rightarrow {}^{87}\mathbf{Sr}(9/2^+)$ **3rd FNU decay** and derive g_A^{eff}.

- **Rb_2ZrCl_6** (RZC) crystal scintillator, mass of 0.4647(1) g → ^{87}Rb present in the natural Rb with $\delta \approx 27.8\%$
- $Q_\beta = 282.275(6)$ keV
- Measured in the low-background DAMA/CRYS setup at LNGS over 22.34 h.
- Energy threshold: 10 keV.
- Activity of ^{87}Rb: ≈ 305 kBq/kg.

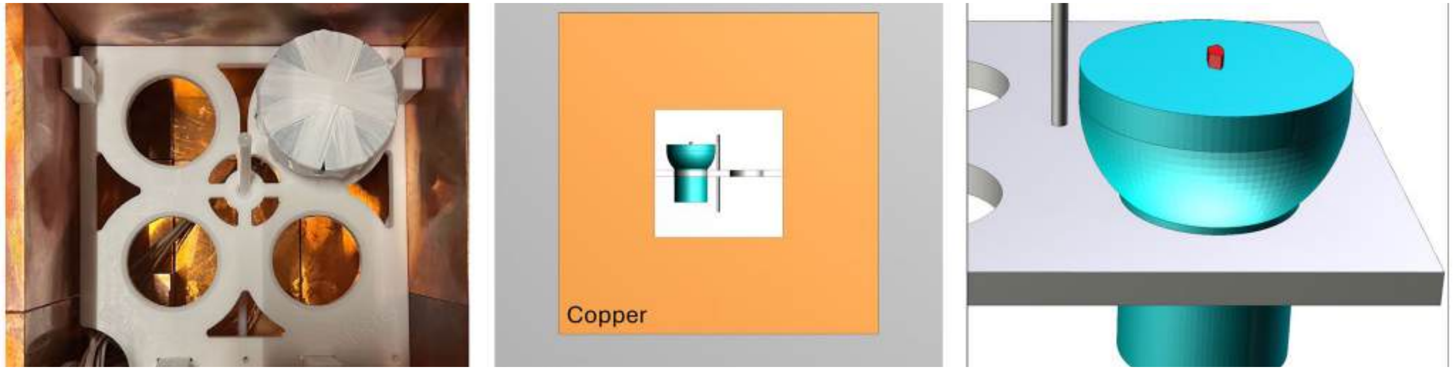

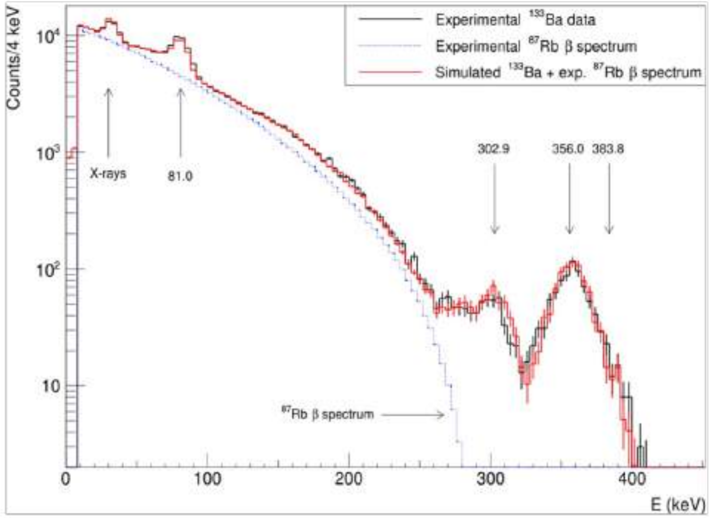

P. Belli et al. EPJA 62(2026) 16

β decay of ^{87}Rb : Results

1. Experimental input

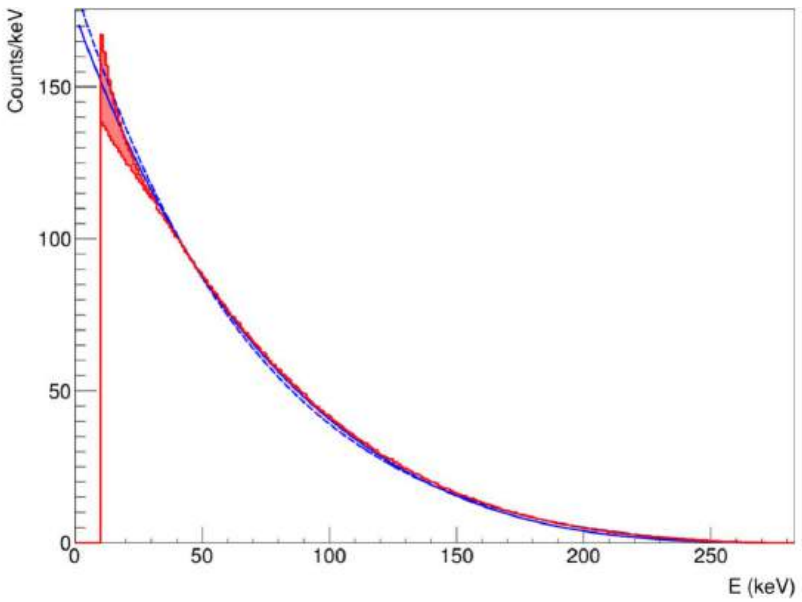

Unfolded ^{87}Rb β spectrum; red band reflects analysis uncertainty below ~30 keV.

$$T_{1/2} = 5.08(13)\times 10^{10}\ \mathbf{yr}$$

P. Belli et al. EPJA 62(2026) 16

2. ESSM comparison with nuclear models

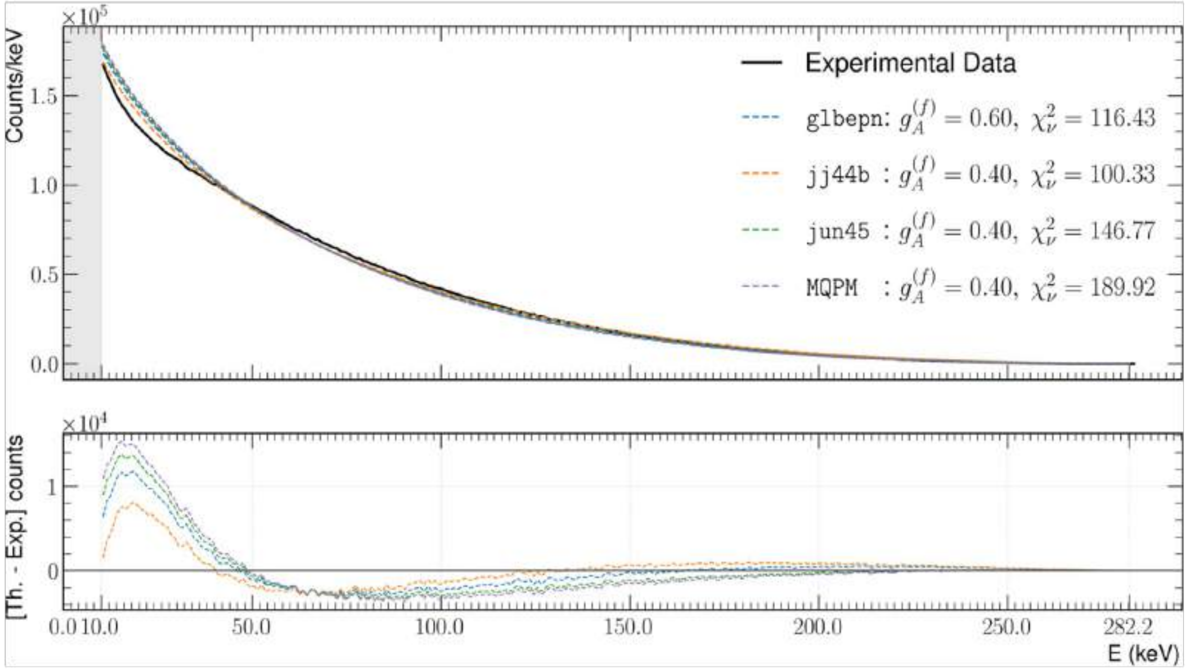

Best-match ESSM spectral shapes for NSM interactions and MQPM; χ^2 minimization selects g_A values.

$$g_A^{eff} \approx 0.40 - 0.60$$

GAIAS scientific perspective

The GAIAS project will focus in sequence on:

- **^{113}Cd** is naturally present in $CdWO_4$ crystal scintillators; **^{113m}Cd** is in the enriched $^{106}CdWO_4$ scintillator

- **^{87}Rb**, and **^{99}Tc**: candidate isotopes for custom crystal-growth R&D. Possible hosts include CsI(Na,Rb), NaI(Tl,Tc) and other Tc-containing compound matrices, pending chemical-feasibility validation.

- R&D for investigating the feasibility of procurement of beta-emitting isotopes such as ^{137}Cs, ^{135}Cs and ^{36}Cl to incorporate as controlled contaminants during crystal synthesis (activity at a level of <100 Bq).

Crystal Scintillator	Beta decay of interest	Feasibility
$CdWO_4$	^{113}Cd	Ready
$^{106}CdWO_4$	^{113m}Cd	Ready
CsI(Na,Rb)	^{87}Rb	Potential (preliminary R&D started)
NaI(Tl,Rb)	^{87}Rb	Potential
NaI(Tl,Tc)	^{99}Tc	Potential
$CeCl_3$	^{36}Cl	Potential
PbI_2	^{210}Bi, ^{214}Bi	Potential
CsI(Tl)	^{135}Cs, ^{137}Cs	Challenging
SrI_2(Eu), CsI	^{129}I	Challenging
…	…	…

- Nuclides present in a scintillator as a result of contamination (natural or artificial) by their parent nuclides (^{210}Bi, ^{214}Bi).

- Feasibility assessment for more challenging isotopes with very short half-lives.

β -transitions of interest sensitive to g_A^{eff}

Transition	Forbidness	Q_β (keV) δ (%)	Half-life	Activity [1]	Possible scintillator, Note
$^{113}Cd \rightarrow ^{113}In$	$1/2^+ \rightarrow 9/2^+$ (100%, 4 FNU)	323.84(27) 12.2227(7)	8.04(5) $\times 10^{15}$ yr	1.8 mBq/g of Cd	$CdWO_4$
$^{113m}Cd \rightarrow ^{113}In$	$11/2^- \rightarrow 9/2^+$ (~100%, 1 FNU)	587.38(27) Synthetic	13.58(32) yr	65-130 mBq/g of $^{106}CdWO_4$	$^{106}CdWO_4$
$^{87}Rb \rightarrow ^{87}Sr$	$3/2^- \rightarrow 9/2^+$ (100%, 3 FNU)	282.275(6) 27.83(2)	4.97(3)$\times 10^{10}$ yr	867 Bq/g of Rb	CsI(Na,Rb), NaI(Tl,Rb)
$^{99}Tc \rightarrow ^{99}Ru$	$9/2^+ \rightarrow 5/2^+$ (100%, 2 FNU)	297.5(9) Synthetic	2.111(12) $\times 10^5$ yr	6.33$\times 10^8$ Bq/g of ^{99}Tc	NaI(Tl,^{99}Tc), CsI(Na,^{99}Tc)
$^{115}In \rightarrow ^{115}Sn$	$9/2^+ \rightarrow 1/2^+$ (100%, 4 FNU)	497.489(10) 95.719(52)	4.41(25) $\times 10^{14}$ yr	0.25 Bq/g of In	CsI(In), $LiInSe_2$, InI
$^{210}Bi \rightarrow ^{210}Po$	$1^- \rightarrow 0^+$ (100%, 1 FNU)	1162.2(8) daughter of ^{210}Pb (^{238}U chain)	5.012(5) d	4.6$\times 10^{15}$ Bq/g of ^{210}Bi	$CaWO_4$, PbI_2
$^{135}Cs \rightarrow ^{135}Ba$	$7/2^+ \rightarrow 3/2^+$ (100%, 2 FNU)	268.70(29) Synthetic	2.3(3)$\times 10^6$ yr	4.3$\times 10^7$ Bq/g of ^{135}Cs	CsI(Tl)
$^{137}Cs \rightarrow ^{137}Ba$	$7/2^+ \rightarrow 3/2^+$ (5.6%, 2 FNU)	1175.63(17) Synthetic	30.04(4) y	3.2$\times 10^{12}$ Bq/g of ^{137}Cs	CsI(Tl)
$^{129}I \rightarrow ^{129}Xe^*$	$7/2^+ \rightarrow 3/2^+$ (100%, 2 FNU)	189(3) (10^{-13}-10^{-12})	1.57(4)$\times 10^7$ yr	0.7-7 μBq/g of I	CsI
$^{36}Cl \rightarrow ^{36}Ar$	$2^+ \rightarrow 0^+$ (98.1%, 2 FNU)	709.53(4) (~7$\times 10^{-13}$)	3.013(15)$\times 10^5$ yr	≈1 mBq/g of Cl	$CeCl_3$
$^{214}Bi \rightarrow ^{214}Po$	$1^- \rightarrow 0^+$ (19.2%, 1 FNU)	3269(11) daughter of ^{226}Ra (^{238}U chain)	19.71(2) min	1.6$\times 10^{18}$ Bq/g of ^{214}Bi	$CaWO_4$, NaI(Tl), CsI(Tl), SrI_2(Eu), $LaCl_3$, ...,
$^{94}Nb \rightarrow ^{94}Mo$	$6^+ \rightarrow 4^+$ (100%, 2 FNU)	2045.0(15) Synthetic	2.03(16)$\times 10^4$yr	6.9$\times 10^9$ Bq/g of ^{94}Nb	Highly effective organic scintillation material with an external synthetic source

[1] specific activity for 1 g of the element in the cases of natural radioactive nuclides, and activity partially to be added to in scintillator in the cases of synthetic elements

Low-background measurement concept at LNGS

Crystal in PTFE container filled with high purity silicone oil

Coupled to two PMTs

Passive shield: 65 cm x 65 cm x 130 cm, composed by 15 cm of Pb, 10 cm Cu

Low-radioactivity in a sealed PTFE box flushed with highly pure N_2

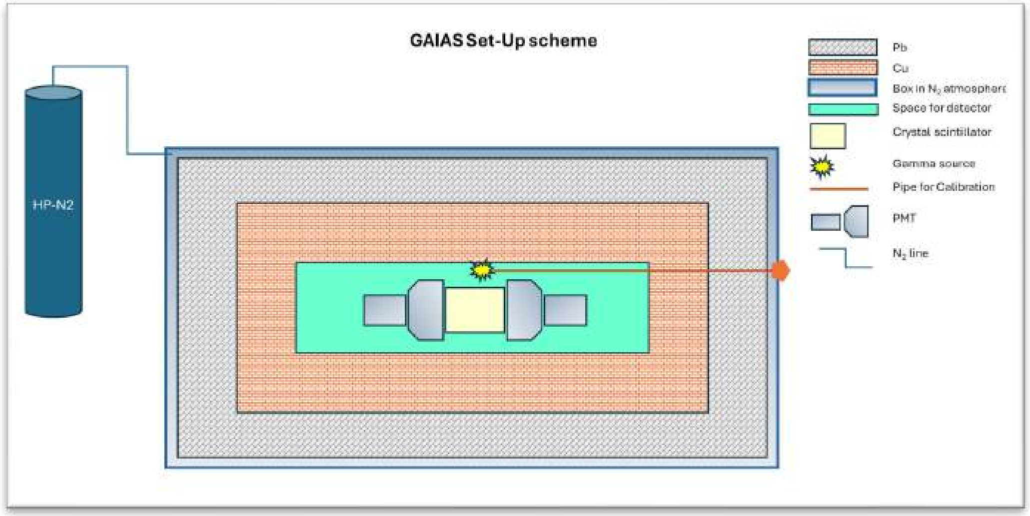

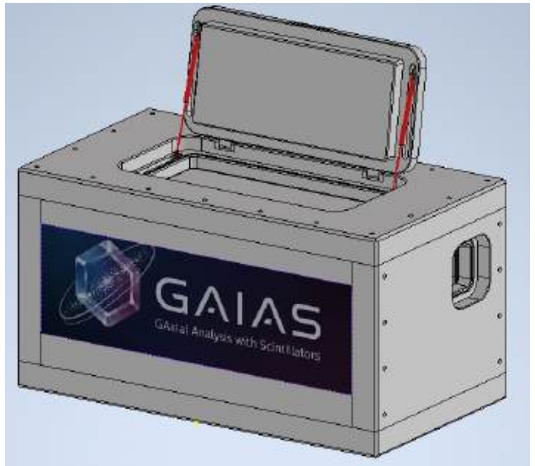

Current experimental status

Work in progress

Hexagonal $CdWO_4$ crystal scintillator to measure ^{113}Cd β spectrum

Hexagonal crystal geometry improves light collection efficiency and uniformity.

Systematic uncertainties control

The accuracy will be limited mainly by systematic effects rather than by statistics.

Energy scale
multiple calibration points across the spectrum, especially in the low-energy region (sources: ^{133}Ba, ^{241}Am, ^{228}Th, ^{226}Ra, ^{57}Co, ^{144}Ce, and ^{109}Cd).

Detector stability
monitored continuously with gamma-sources inserted through the special pipe to correct for gain drifts and environmental effects.

Background model
validated through dedicated runs and compared with Monte Carlo simulation.

Project high-level timeline

2026

Detector development

crystal growth and characterization; test of scintillators and first measurement of $CdWO_4$; isotopes procurement; R&D start

2027

Measurement campaign

sequential data acquisition at LNGS, about one month per selected crystal

2028

Data analysis and dissemination

spectral-shape analysis extraction of g_A^{eff} and publications

Collaboration

Institution	Name	Position
INFN–Roma Tor Vergata (Italy)	Riccardo Cerulli (PI) Vincenzo Caracciolo Pierluigi Belli Alice Leoncini Mattia Atzori Corona Vittorio Merlo Andrea Bussolotti	Senior Researcher Associate Professor Director of research Post-doc Tor Vergata University Post-doc INFN Former Senior Lecturer INFN Technician
INFN–Roma Sapienza (Italy)	Fabio Cappella (PI Roma1) Antonella Incicchitti Alessio Giarnetti Angelo Mattei	Senior Researcher Director of research Post-doc INFN INFN Technician
INR–Kyiv (Ukraine)	Fedor Danevich (PI) Volodymyr Tretyak Vladislav Kobychev Dmytro Kasperovych Volodymyr Klavdiienko	Director of research Director of research Director of research Senior Researcher Junior Researcher
University of Jyväskylä (Finland)	Jouni Suhonen (PI) Jenni Kotila Aagrah Agnihotri Marlom Ramalho	Full Professor Senior Researcher PhD student Post-doc

Conclusions

- ✓ The determination of g_A^{eff} is crucial for the interpretation of weak nuclear processes and $0\nu\beta\beta$ searches.
- ✓ GAIAS can measure the g_A^{eff} value with high precision for various isotopes by using crystal scintillators and exploring novel approaches.
- ✓ The experimental technique is well established, as demonstrated by previous scintillation measurements and ongoing R&D activities.
- ✓ The collaboration brings together all the necessary expertise and experience to achieve the proposed goals.
- ✓ The project will run for 3 years at LNGS.

BACKUP

Spectral shape of forbidden non-unique β decays

$$T_{1/2} = \kappa/\tilde{C}$$

$$\kappa = \frac{2\pi^3\hbar^7 \ln 2}{m_e^5 c^4 (G_F \cos\theta_C)^2} = 6147\ \mathrm{s},$$ is a constant and θ_C is the Cabibbo angle;

$$\tilde{C} = \int_1^{w_0} C(w_e) p w_e (w_0 - w_e)^2 F_0(Z_f, w_e) dw_e$$ is the dimensionless integrated shape function;

$$C(w_e) = \sum_{k_e, k_\nu, K} \lambda_{k_e} \left[M_K(k_e, k_\nu)^2 + m_K(k_e, k_\nu)^2 - \frac{2\gamma_{k_e}}{k_e w_e} M_K(k_e, k_\nu) m_K(k_e, k_\nu) \right],$$ is the general form of the shape factor for forbidden β decays;

where $$\lambda_{k_e} = \frac{F_{k_e - 1}(Z, w_e)}{F_0(Z, w_e)}; \quad \gamma_{k_e} = \sqrt{k_e^2 - (\alpha Z_f)^2},$$

$F_{k_e-1}(Z, w_e)$ is the generalized Fermi function; k_e and k_ν come from the partial-wave expansion of the electron and neutrino wave function

Decomposition of the shape factor:

$$C(w_e) = g_V{}^2 C_V(w_e) + g_A{}^2 C_A(w_e) + g_V g_A C_{VA}(w_e)$$

Nuclear Models

ISM / Shell Model

- exact diagonalization
- strong correlations in a restricted valence space
- excellent spectroscopy
- limited orbitals

pnQRPA

- large single-particle spaces
- proton-neutron quasiparticle excitations
- sensitive to gpp and pairing strength

Ab initio

- From chiral EFT interactions and currents; aims at controlled uncertainties and less phenomenology.
- Powerful benchmark but still limited for many medium-heavy $0\nu\beta\beta$ candidates

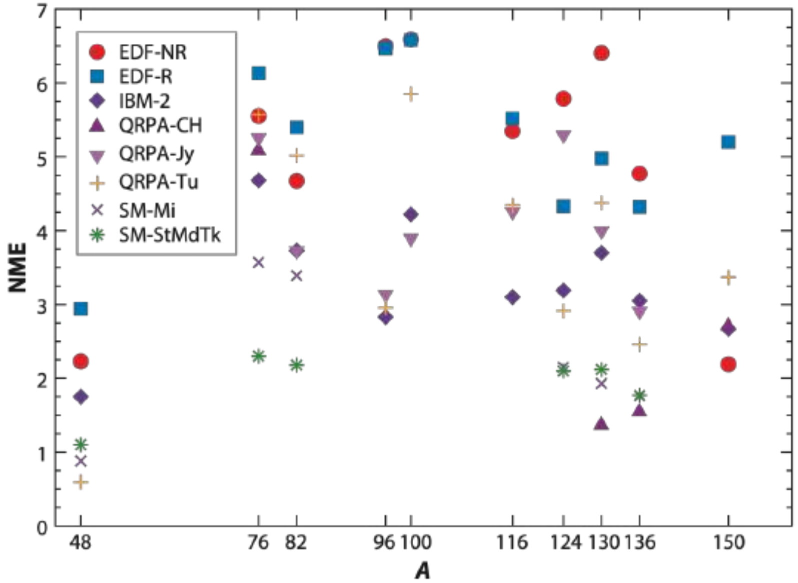

J.M. Dolinski et al, Annu. Rev. Nucl. Part. Sci. 2019. 69:219–51

IBM-2 / IBFFM-2

- maps correlated nucleon pairs to bosons
- efficient for collective and heavy nuclei
- more phenomenological, compact space

EDF / PHFB

- mean-field with deformation and pairing
- large spaces; global trends
- correlations restored approximately

more exact correlations → larger model spaces

Stages of the low-background measurements at LNGS – β decay of ^{113m}Cd

Stage of experiment	1	2	3
Measurement dates	09 – 23 Nov 2009	30 Apr – 19 May 2015	20 Sep – 05 Oct 2023
Specific modifications	Reference setup with quartz light guides and original electronics [6]	Crystal etched to remove ^{207}Bi surface contamination [7,8]	Quartz light guides removed; new low-background Hamamatsu PMTs; improved light collection efficiency [8]
Live time (h)	248.0(10)	392(6)	340.9(34)
Mass of $^{106}CdWO_4$ crystal scintillator (g)	215.8	215.4	215.4
Energy resolution at 587 keV (σ, keV)	31.1(2)	31.8(4)	23.2(3)
Energy threshold accepted in analysis (keV)	39	64	26
Background in (0.8 – 2.0) MeV (counts/day)	66(2)	119(3)	105(2)
Signal-to-background ratio in (100 – 580) keV	549	398	294

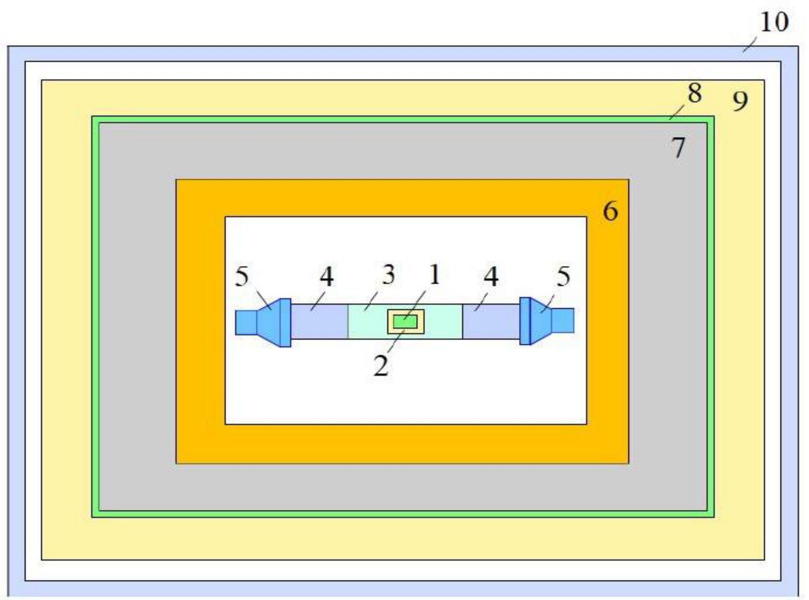

Schematic cross-sectional view of the experimental set-up used to measure ^{113m}Cd β spectrum in 2009. The $^{106}CdWO4$ crystal scintillator (1) is fixed in a cavity filled by silicon oil (2) inside polystyrene plastic light guide (3) and viewed through quartz light guides (4) by PMTs (5). The passive shield consisted of high-purity copper (6), low-radioactive lead (7), cadmium (8), polyethylene/paraffin (9), and a poly(methyl methacrylate) box flushed with N_2 gas (10).

[6] P. Belli et al., Phys. Rev. C 85 044610 (2012) .
[7] P. Belli et al., Phys. Rev. C.93 045502 (2016).
[8] Present study